Multipurpose Antenna Array for Backscattering, Reconfigurable Intelligent Surfaces and MIMO Communications

Abdelwaheb Ourir, Dinh-Thuy Phan-Huy, Philippe Ratajczak, Julien de Rosny

Multipurpose Antenna Array for Backscattering, Reconfigurable Intelligent Surfaces and MIMO Communications

Abdelwaheb Ourir*, Dinh-Thuy Phan-Huy†, Philippe Ratajczak†, and Julien de Rosny*
*ESPCI Paris, PSL Research University, CNRS, Institut Langevin, 1 rue Jussieu, F-75005 Paris, France, a.ourir@espci.fr
†Orange Labs Networks, Chatillon, France

***Abstract*—Energy consumption of mobile network is a major issue. One solution is to use antenna arrays to focus RF field on the receiver. But recently two other techniques have been also proposed. First the RIS are programmable mirrors which can be used to redirect a RF wavefront emitted by a source toward one or several receivers. Second the ultra-low power backscattering devices recycle the ambient RF field to transmit information. Actually, the best energy aving approach depends on many different parameters. So here we propose a multipurpose antenna array (MAA) able to manage these three operating modes simultaneously. The MAA switches between the different modes thanks to an electronic circuit made of PIN diodes. We propose a simple model of MAA based on impedance analysis. Finally, we evaluate experimentally the performances of the three operating modes of a MMA made of 4 patch antennas working at 3.7 GHz.**

***Index Terms*—Backscatter communication, MIMO, radio-frequency, electromagnetic waves.**

I. Introduction

The energy consumption of communication systems keeps increasing due to the fast growth of the number of connected devices by every mobile network generation. As a consequence, it becomes a major issue for the 5G and the next generations of telecommunication systems. One solution can come from the introduction of massive MIMO devices. Indeed, thanks to its beamforming ability, an antenna array can concentrate the energy on a receiver even in a complex environment such as a room[1]. However, the complexity of such systems makes that the energy saving not always sufficient. To overcome this limitation, recently reconfigurable intelligent surfaces (RIS) have been proposed. These surfaces are composed of hundreds of small reflectors whose phase can be tuned electronically. They can be used to shape the electromagnetic environment and focus the signal transmitted by an emitter on a receiver. This effect has been demonstrated in a room[2] and seems very promising for the next generation of telecommunication systems[3]. Finally, one can even do communication without emitting a RF carrier using backscatter communication systems. It has been proposed as a promising low-energy technology for the Internet of Things [4]. In such a system, a backscattering device, the tag, is able to transmit binary messages to a receiver, the reader, by modulating the propagation channel between a radio frequency (RF) source and the reader. Usually, the modulated Radio-Frequency (RF) waves are generated by existing ambient sources such as a TV tower, Wi-Fi hot-spot or 5G base station.

All these solutions are complementary to each other. Indeed, MIMO solutions are adapted for high-rate, long-range communications. Reconfigurable surfaces are more adapted for low power, intermediate rates and long distance communications because it does not take the benefit of channel diversity. Finally, the backscattering is more suited for a low rate, short-range communication.

Here we propose a multipurpose antenna array (MAA) that is able to manage these three operating modes. The cornerstone of MAA is the switching device that allows commuting between the different modes. This device is described in the next section. Then we introduce a simple model based on the computation of the self and mutual impedances between dipoles to assess the effect of the operating modes on the propagation channel between an emitter and a receiver. Finally, we present an experimental demonstration of such an MAA with an array of 4 patches working at 3.7 GHz.

II. Design of switching device

A MAA that is able to handle backscattering communications and conventional communications, and potentially MIMO communications, should be capable of enabling the selected type of communication through a switching circuit for the different modes. Here, we propose to take advantage of the fast switching ability of radio-frequency (RF) PIN diodes combined with the microstrip technology in order to design a compact and efficient version the desired MAA.

The electric model of the designed tag is presented in Fig. 1(a). A main circuit composed of transmission lines and 2 PIN diodes. A schematic view of the microstrip circuit implementation of this main circuit is illustrated in Fig. 1(b). The phase of the backscattered signal is dependent on the state of the PIN diode 1. The signal is reflected by an open circuit at the diodes interconnection when the diode 1 is OFF, while this signal is reflected by an open circuit at the end of the $\lambda/4$ line when the diode 1 is enabled. Thereby, a phase shift of 180? is imposed on the reflected signal when the diode 1 is ON compared to the OFF situation. Furthermore, when the diode 2 is enabled and the diode 1 is blocked, the RF signal goes directly to the transceiver without reflection.

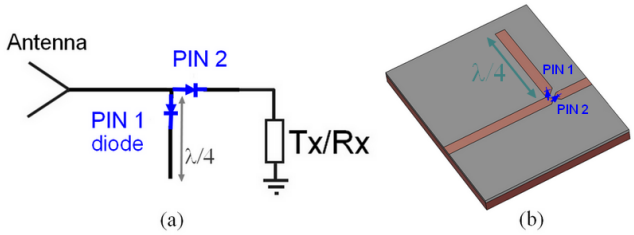

Fig. 1. (a) Electric model of the Rx/Tx/backscattering tag. (b) Schematic view of the microstrip circuit implementation. The 4 V and 0 V voltage correspond respectively to the ON and OFF states for the diodes.

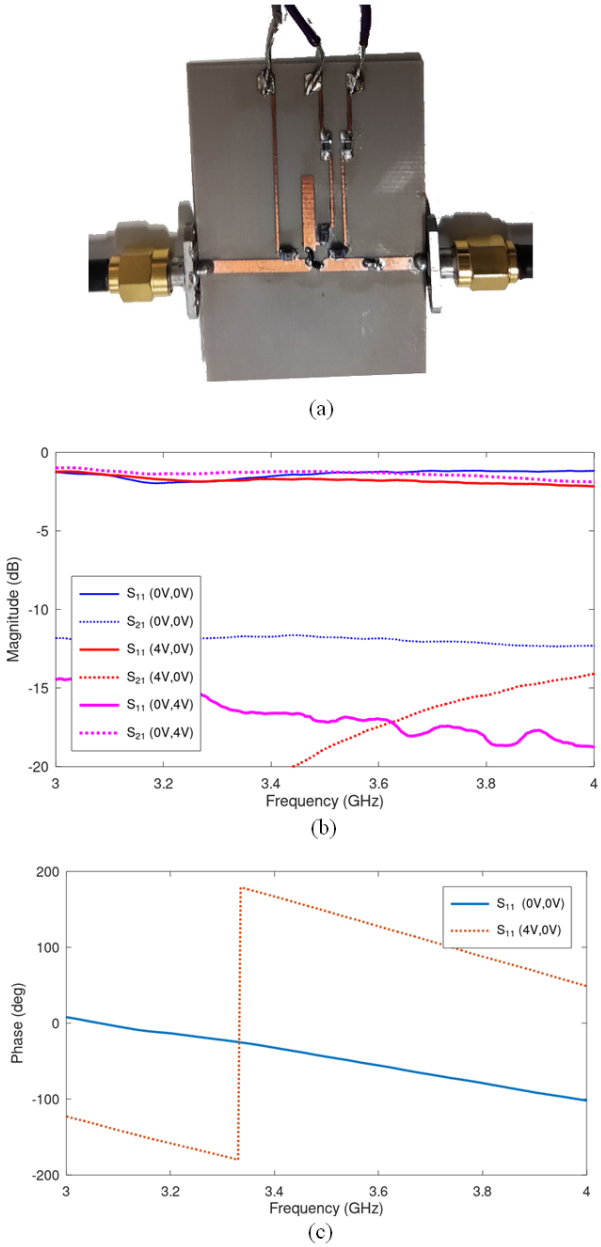

Fig. 2. (a) Photography of the main switching circuit. Magnitudes (b) and phases (c) of the measured s-parameters of the circuit.

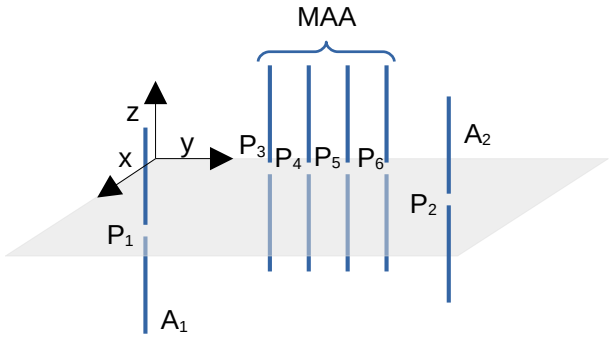

Fig. 3. Schematic view of the linear antenna array configuration.

A prototype of the main switching circuit is realized on a 0.8-mm-thick Duroid substrate. Fig. 2(a) shows a photography of this prototype. S-parameter measurements are performed to characterize the realized circuit using a Vector Network Analyzer (VNA). The measured magnitudes of the transmission and reflection coefficients for the different states are presented in Fig. 2(b). The curves of the backscattering mode correspond to the cases where the 0 V voltage is applied on the diode 2. Satisfactory losses of of 1.2 and 1.8 dB are obtained at 3.7 GHz on the reflection coefficient for the backscattering mode respectively for the ON (4 V) and OFF (0 V) states of diode 1. A reasonable isolation on the second port is observed in both situations. The transmit mode is obtained by applying 4V on diode 2 and 0V on diode 1. In this configuration, a satisfactory transmission coefficient magnitude of -1.5 dB at 3.7 GHz is achieved. Finally, a constant phase shift of about 180^o is observed over a relatively wideband around 3.7 GHz between the reflection coefficient of the two reflecting states as shown in Fig. 2(c). These states are intended to generate the 2 backscattered signal phase-shifted of 180^o of the backscattering mode.

III. Model of MAA

In order to investigate the basic properties of our communication system, we propose to consider simple dipole antennas for the source, the readers and also for the antennas of the MAA. To simplify the modeling, all these linear omni-directional antennas are vertically polarized (see Fig. 3). Because the mutual coupling between antennas cannot be ignored if the antennas are near each other, we propose to implement the thin wire impedance model for linear antenna arrays presented in Ref. [5]. For a given spatial distribution of the dipoles, the matrix $\boldsymbol{Z}_A$ composed of the self and mutual impedance between all the dipole ports (e.g., 6 in Fig. 3) is computed. The load impedances of the emitter, the receiver and the MAA dipoles but in transmitting mode are set to 50Ω. In reflection mode, the impedances of MAA become equal to

$$Z_L \quad = j \quad Z_s \text{cotan}(k_0 d),$$

where d and Z_s are the length and the impedance of the microstrip line, respectively in reflection mode. Note that when

Index	0	1	2
State	Reflective 0?	Reflective 180?	Transmission to USRP

TABLE I
THE INDEX OF THE STATES OF THE SWITCH DEVICE.

the PIN diode is switched "on", the length d is increased by a quarter wavelength and Z_L equals 50Ω. The load impedances are gathered in a diagonal matrix $\boldsymbol{Z}_L$. The currents in all the dipoles can be then deduced from the inversion of the square symmetric matrix $\boldsymbol{Z}_A + \boldsymbol{Z}_L$, i.e., from

$$\boldsymbol{I} = (\boldsymbol{Z}_A + \boldsymbol{Z}_L)^{-1}\boldsymbol{V},$$

where $\boldsymbol{V}$ is a vector regrouping driving voltages. Only the driving voltage of an emitting antenna is different from 0.

IV. Numerical results

We apply the previous model to characterize the behavior of our MMA in the case it is composed of a single antenna where the load impedance is switched between the three states shown in Tab. I. Fig. 4(a) shows the geometric configuration. The Rx antenna is placed at a distance of 20 cm of the Tx antenna. We calculate the signal level on the receiver for the different MMA states and positions along the x-axis. Fig. 4(b) and (c) present the results when $d = 0$, i.e., when the reflection does not induce any phase shift ($\phi = 0$) and in the presence of a phase shift ϕ of 180? due to the fact that $d = \lambda/4$. One can notice that in the first case ($\phi = 0$), the device is equivalent to the conventional ON/OFF backscatter by toggling between a transparency state ($Z = \infty$: blue curve) and a scattering state ($Z = 0$: red curve) to incident RF waves. An intermediate state is observed when the tag is in the Tx/Rx mode ($Z = 50$). The strong oscillations of the signals in the last two configuration result from interference effects between the direct path between the source and the receiver and the path that is scattered by the MMA.

In practice, we are not able to control the absolute phase of ϕ. Due to the coax cables, the microstrip lines, etc. an arbitrary constant phase shift φ should also be taken into consideration. In Fig. 4(c) and extra phase shift of 90? that would correspond to a length of $\lambda/8$ has been taken into account. We can observe that the relative level difference between the states $\phi = 0°$ and $\phi = 180°$ is now smaller implying a less efficient amplitude modulation.

V. Experimental validation

We have built a prototype of MAA composed of 4 antenna patches vertically polarized. The pitch of the array is 45 mm and the central frequency of the patches is 3.7 GHz. Each patch is connected to its own switching device described in Sec. II. All the switches are driven by the same microcontroller. The output port of the switching devices are connected to the Rx channels of two B210. These Universal Software Radio Peripherals (USRP) are provided by National Instruments. A patch antenna and a dipole antenna are connected to the Tx/Rx channels to 2 others USRPs. The two last channels are used

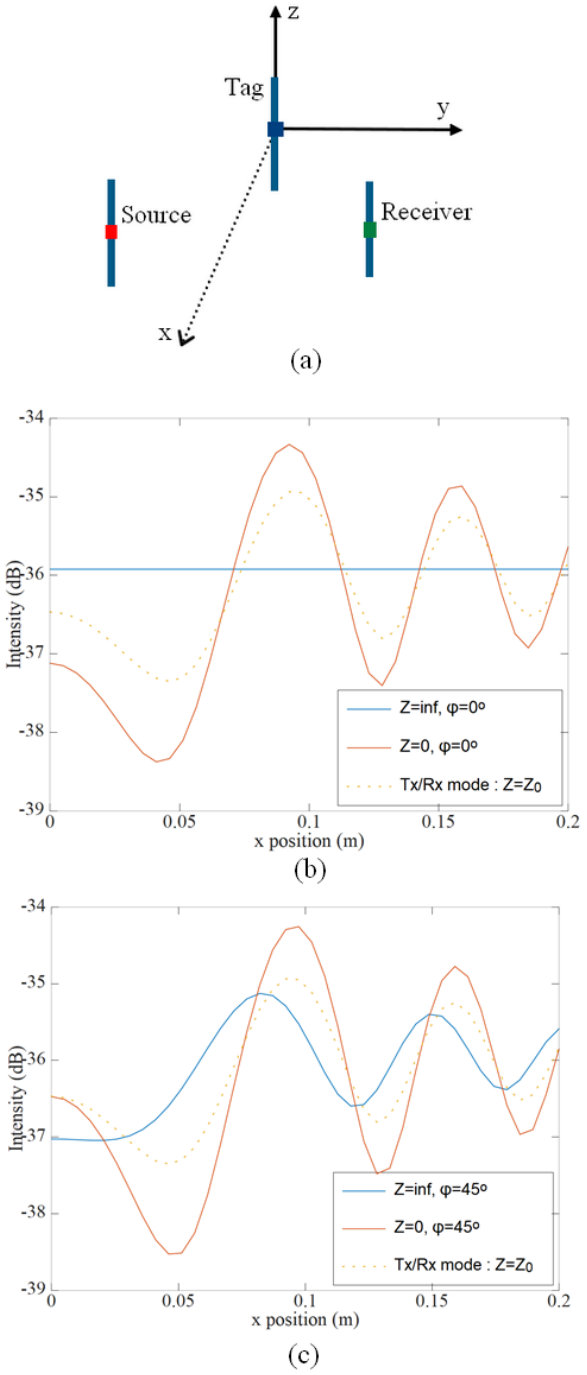

Fig. 4. (a) Schematic view of the communication configuration. The tag is moving along the x-axis. The calculated receiver signals for the different modes of the tag with (b) and without (c) the cable phase shift effect.

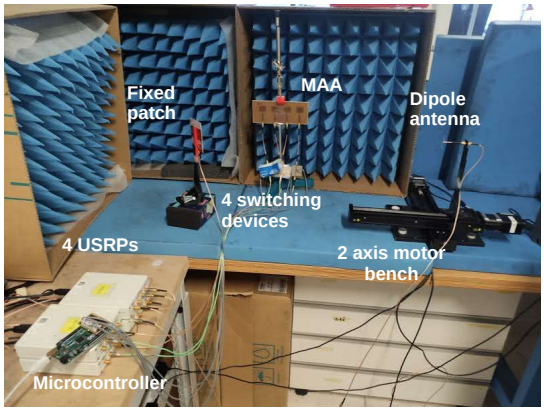

Fig. 5. Photography of the setup.

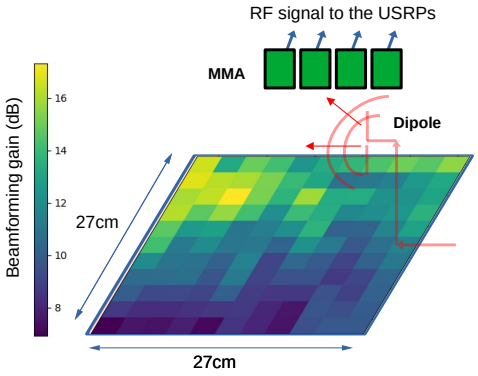

Fig. 6. Beamforming post-processing gain (see text) when the dipole is emitting at 3.7 GHz for different positions of the dipole.

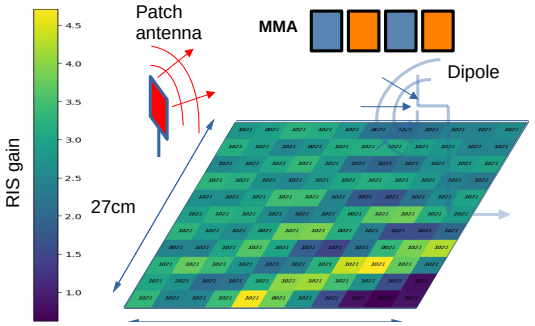

Fig. 7. RIS gain (see text) for a patch antenna emitting at 3.7 GHz and transmitting information to the dipole.

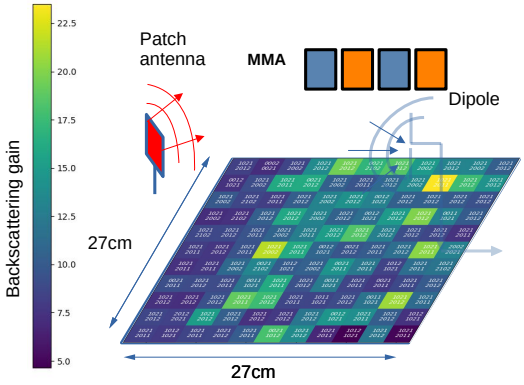

Fig. 8. Backscatter gain (see text) for a patch antenna emitting at 3.7 GHz. The patch antenna plays the role of the ambient source and the MAA transmit by amplitude modulation data to the dipole.

to check the phase stability of the USRPs. The USRPs are synchronized by a common reference 100 MHz signal. The dipole antenna is mounted on a 2-axis motor bench. Gnuradio software is used to monitor the 4 USRPs. In its current form, the setup allows acquiring the channel responses between the patch (respect. dipole antenna), the dipole antenna (respect. path antenna) and the four antennas of MAA. From these responses, we have computed 3 quantities to evaluate the efficiency of the MAA in the 3 different operating modes. First, for a simple conventional input multiple output (SIMO) communication mode between the dipole and the MMA, we have computed the gain provided by a post-processing beamforming. The gain is given by

$$G = 10\log_{10}\left(\frac{\sum_{i=1}^{4}|H_i|^2}{|H_1|^2}\right)$$

where H_i is the complex amplitude probed by the i-th antenna of the MAA when the dipole emits a continuous wave. We can observe in Fig. 6.The values of the gain range between 7dB and 17dB. Second, we test the MAA as a RIS. To that end while the patch antenna emits a continuous wave, the maximum intensity probed by the dipole antenna is worked out from the 3^4 configurations of the MAA states.

On Fig. 7, we have plotted the RIS gain as the ratio of this maximum over the intensity when all the switching devices are in state 0 for different position of the receiver. We observe that for some positions of the receiver, the RIS provides an enhancement of a factor up to 6dB. Most of the time the best configuration state is 1021 (state index of the first, second, third and fourth antennas). Note that in that case the third antenna is absorptive.

Finally, we have tested the efficiency of the MAA to perform backscattering. To that end we have computed from 3^8 configurations, the 2 configurations that provide the maximum difference of intensities, i.e., the 2 configurations with the highest amplitude modulation factor. Then we compute the backscattering gain as the ratio of this highest difference of intensities over the difference of intensities between the states 0000 and 1111. The results are shown in Fig 8. Once again we observe that the two best configurations are most of the time 1021 associated to 2011. Note that this result is coherent with the previous one with the maximum intensity. The state 2011 is the state that induces the minimum intensity on the receiver.

VI. Conclusion

We have designed an original array that is able to switch between 3 different operating modes. Hence, this is a unique

tool in order to survey the links between MIMO, RIS and backscattering. Indeed as we have seen in the experimental part, the best RIS configuration is closely related to an optimal backscatter configuration. Moreover up to now, the best backscatter configuration is obtained using a time consuming iterative optimization algorithm that is not compatible with mobile communications. This setup allow to test in practice whether the acquisition of the MIMO channel can help the finding of the optimal RIS configuration.

ACKNOWLEDGMENT

This work is supported by LABEX WIFI (Laboratory of Excellence within the French Program Investments for the Future) under references ANR-10-LABX-24 and ANR-10-IDEX-0001-02 PSL*.

REFERENCES

[1] L. Lu, G. Y. Li, A. L. Swindlehurst, A. Ashikhmin, and R. Zhang, "An overview of massive mimo: Benefits and challenges," *IEEE journal of selected topics in signal processing*, vol. 8, no. 5, pp. 742–758, 2014.

[2] G. Lerosey, J. de Rosny, A. Tourin, and M. Fink, "Focusing beyond the diffraction limit with far-field time reversal," *Science*, vol. 315, no. 5815, pp. 1120–1122, 2007. [Online]. Available: http://www.sciencemag.org/content/315/5815/1120.abstract

[3] M. D. Renzo, M. Debbah, D.-T. Phan-Huy, A. Zappone, M.-S. Alouini, C. Yuen, V. Sciancalepore, G. C. Alexandropoulos, J. Hoydis, H. Gacanin *et al.*, "Smart radio environments empowered by reconfigurable ai meta-surfaces: An idea whose time has come," *EURASIP Journal on Wireless Communications and Networking*, vol. 2019, no. 1, pp. 1–20, 2019.

[4] V. Liu, A. Parks, V. Talla, S. Gollakota, D. Wetherall, and J. R. Smith, "Ambient backscatter," in *Proceedings of the ACM SIGCOMM 2013 conference on SIGCOMM*. ACM, aug 2013. [Online]. Available: https://doi.org/10.1145-2F2486001.2486015

[5] S. J. Orfanidis, *Electromagnetic Waves and Antennas*. ECE Department, Rutgers University, 2016. [Online]. Available: https://www.ece.rutgers.edu/ orfanidi/ewa/